The Inositol 1,4,5,-Trisphosphate Receptor in Cerebellar Purkinje Cells: Quantitative Immunogold Labeling Reveals Concentration in an ER Subcompartment

Tomohide Satoh,* Christopher A. Ross,‡ Antonello Villa,* Surachai Supattapone, Tullio Pozzan,§ Solomon H. Snyder,‡ and Jacopo Meldolesi*

*Department of Pharmacology, Consiglio Nazionale delle Ricerche Center of Cytopharmacology, Bruno Ceccarelli Center for Peripheral Neuropathies and S. Raffaele Institute, University of Milan, 20132 Milan, Italy; ‡Department of Neurosciences, Pharmacology, and Molecular Sciences, Psychiatry and Behavioral Sciences, Johns Hopkins University School of Medicine, Baltimore, Maryland 21205; and §Institutes of General Pathology, University of Ferrara, 44100 Ferrara, Italy

Abstract. The Ca^{2+} mobilization effect of inositol 1,4,5-trisphosphate, the second messenger generated via receptor-stimulated hydrolysis of phosphatidylinositol 4,5-bisphosphate, is mediated by binding to intracellular receptors, which are expressed in high concentration in cerebellar Purkinje cells. Partially conflicting previous reports localized the receptor to various subcellular structures: elements of ER, both rough and smooth-surfaced, the nuclear envelope, and even the plasma membrane. We have now reinvestigated the problem quantitatively by using cryosections of rat cerebellar tissue immunolabeled with polyclonal monospecific antibodies against the inositol 1,4,5-trisphosphate receptor. By immunofluorescence the receptor was detected only in Purkinje cells, whereas the other cells of the cerebellar cortex remained negative. In immunogold-decorated ultrathin cryosections of the Purkinje cell body, the receptor was concentrated in cisternal stacks (piles of up to 12 parallel cisternae separated by regularly spaced bridges, located both in the deep cytoplasm and beneath the plasma membrane; average density, >5 particles/μm of membrane profile); in cisternal singlets and doublets adjacent to the plasma membrane (average density, ≈2.5 particles/μm); and in other apparently smooth-surfaced vesicular and tubular profiles. Additional smooth-surfaced elements were unlabeled. Perinuclear and rough-surfaced ER cisternae were labeled much less by themselves (≈0.5 particles/μm, two- to threefold the background), but were often in direct membrane continuity with heavily labeled, smooth-surfaced tubules and cisternal stacks. Finally, mitochondria, Golgi cisternae, multivesicular bodies, and the plasma membrane were unlabeled. In dendrites, approximately half of the nonmitochondrial, membrane-bound structures (cisternae, tubules, and vesicles), as well as small cisternal stacks, were labeled. Dendritic spines always contained immunolabeled cisternae and vesicles. The dendritic plasma membrane, of both shaft and spines, was consistently unlabeled. These results identify a large, smooth-surfaced ER subcompartment that appears equipped to play a key role in the control of Ca^{2+} homeostasis: in particular, in the generation of $[Ca^{2+}]^i$ transients triggered by activation of specific receptors, such as the quisqualate-preferring trans(±)-1-amino-1,3-cyclopentamedicarboxylic acid glutamatergic receptors, which are largely expressed by Purkinje cells.

STUDIES carried out in many laboratories since 1982 have documented the key physiological role of inositol 1,4,5-trisphosphate ($InsP_3$)[1] in the control of intracellular Ca^{2+} homeostasis. This second messenger, generated via receptor-activated hydrolysis of phosphatidylinositol 4,5-bisphosphate, is responsible for Ca^{2+} release from an intracellular, rapidly exchanging membrane-bound store that appears to be expressed by all eukaryotic cell types (for a recent review see Berridge and Irvine, 1989). The intracellular receptor that mediates the effect of $InsP_3$, $InsP_3R$, initially hypothesized on the basis of binding studies (Spät et al., 1986; Guillemette et al., 1987*a*,*b*), was purified from the rat cerebellum in one of our laboratories and found to correspond to a 260-kD phosphoprotein (Supattapone et al., 1988*a*). The receptor was independently identified as a Purkinje cell–selective protein, designated P400 (Mallet et al., 1976; see also Groswald and Kelly, 1984; Walaas et al., 1986). In the brain the $InsP_3R$ is highly concentrated in cerebellar Purkinje cells and in a few other neuronal types,

1. *Abbreviations used in this paper*: $InsP_3$, inositol 1,4,5-trisphosphate; $InsP_3R$, inositol 1,4,5,-trisphosphate receptor.

whereas in other brain regions and in many peripheral tissues its levels are much lower (Worley et al., 1989; Supattapone et al., 1988*b*; Ross et al., 1989; Furuichi et al., 1989; Mignery et al., 1989). Reconstitution studies have revealed that this receptor molecule includes the ion channel activated by $InsP_3$ binding (Ferris et al., 1989), a conclusion that appears compatible also with the recently reported primary structure of the protein (Furuichi et al., 1989; Mignery et al., 1989).

Several groups have recently carried out immunocytochemical localizations of the $InsP_3R$ at the light and electron microscopic level. Using an affinity-purified polyclonal Ab against the rat brain $InsP_3R$, we found peroxidase immunoreactivity in the soma and dendrites of Purkinje cells, on rough and smooth ER and nuclear membranes, but no label on mitochondria or plasma membrane (Ross et al., 1989). By contrast, using monoclonal Abs directed against the P400 protein, Maeda et al. (1989) found label on ER and also plasma membrane. Mignery et al. (1989), on the other hand, used an Ab raised against a peptide sequence in the $InsP_3R$. When this Ab was applied to cerebellum homogenates that were then immunodecorated with colloidal gold particles, specific labeling was found on smooth ER elements and also on hypolemmal cisternae, but not on rough ER and the plasma membrane. None of these studies used quantitative analysis to compare the labeling of these different structures. We have now undertaken a quantitative EM immunocytochemical study of the distribution of $InsP_3R$ in rat Purkinje cells.

Using gold-immunolabeled ultrathin cryosections, we demonstrate that smooth cisternae, often arranged in parallel stacks, as well as smooth tubules, possess high levels of immunoreactive $InsP_3R$, both in the cell body and the dendritic tree up to the dendritic spines. Rough-surfaced ER cisternae and the nuclear envelope are less labeled on their own, but can be in direct lumenal continuity with heavily labeled smooth elements. Hypolemmal cisternae are most often labeled to an intermediate degree. By contrast, no specific label is detected on mitochondria, the nucleus or the plasma membrane.

Materials and Methods

Materials

Rabbit polyclonal anti-rat cerebellum $InsP_3R$ and preimmune antisera were described by Ross et al. (1989) and Supattapone et al. (1988*a*). Abs immunopurified from the anti $InsP_3R$ serum were used as such or after preincubation with excess purified antigen (Ross et al., 1989). Rhodamine-labeled anti-rabbit IgGs were purchased from Seralab-Technogenetics (Milan, Italy); protein A-coated 5-nm colloidal gold particles were purchased from Janssen, Pharmaceutica (Beerse, Belgium). Other chemicals were analytical or the highest grade available.

Conventional and Immuno Microscopy

Male 100–150-g rats were anesthetized with thiopenthal and then perfused through the heart, first with 200 ml PBS at 4°C and then with a mixture of 4% formaldehyde (freshly prepared from paraformaldehyde) and 0.2% glutaraldehyde in 125 mM phosphate buffer, pH 7.4 (500 ml, at 4°C). The cerebellum was rapidly removed and ≈1-mm-thick frontal slices were prepared. The slices were immersed into the fixative mixture and then sectioned into squares. Those including the boundary between the molecular and granular layers of the cortex were further fixed in the same mixture for 2 additional h and then processed for both conventional microscopy and immunocytochemistry.

Samples for conventional EM were washed extensively with the phosphate buffer, postfixed with 1% OsO_4 in 125 mM cacodylate buffer, dehydrated in ethanol, block-stained with uranyl acetate, and embedded in Epon. Thin sections were double-stained with uranyl acetate and lead citrate. The samples for cryosections were infiltrated with concentrated sucrose, frozen in Freon 12 cooled with liquid nitrogen, and transferred to an ultramicrotome (Ultracut; Reichert Jung, Vienna, Austria) equipped with a FC_4 cryosection apparatus. 1-μm thick sections were flattened over glass slides and covered with 2% liquid gelatin in phosphate buffer. After a short treatment with 1% Na borohydrate, the sections were washed and exposed for 30 min to a normotonic solution containing 0.5% Triton X-100, 30% filtered goat serum, 0.9% NaCl, and 10 mM phosphate buffer, pH 7.4. After being washed, the samples were exposed (1 h at 37°C or overnight at 4°C) to either the anti-$InsP_3R$ or the corresponding preimmune Abs diluted in the solution described. Sections were then washed again thoroughly and treated with rhodamine-labeled goat anti-rabbit Abs (1/20–1/40 in the Triton X-100–goat serum solution, 30–60 min, 37°C), washed again and mounted in glycerol to the examined in a Zeiss Photomicroscope III apparatus.

For immunogold, ultrathin cryosections (≈100 nm) were collected over nickel grids and covered with 2% gelatin. After treatment with 125 mM phosphate buffer, pH 7.4, supplemented with 0.1 M glycine, they were exposed to the first Ab for 1 h at 37°C, (anti-$InsP_3R$ or preimmune, diluted in phosphate-glycine buffer) and then washed with phosphate-glycine buffer and decorated with protein A-coated gold particles (5 nm, dilution 1/80 in the same buffer). The immunodecorated grids were then washed and processed as recommended by Keller et al. (1984). For additional details see Hashimoto et al. (1988). Both conventional sections and cryosections were examined in a Hitachi H-7000 electron microscope. Pictures were usually taken at a magnification of 24,000.

Specificity and Quantitative Evaluation of Immunogold Labeling

With preimmune serum the gold labeling of cryosections was low and uniformly distributed over the Purkinje cell nucleus and cytoplasm as well as over the adjacent cells. The average labeling, calculated under standard conditions in a group of randomly chosen pictures, i.e., the background, was 4.8 gold particles/μm^2. With anti-$InsP_3R$ Abs (immune serum and affinity-purified Abs) the labeling of various structures within Purkinje cells (described below) was distinctly above background, whereas the nucleus and the mitochondria were not significantly different from the background. In other cells of the cerebellar cortex, the labeling with the anti-$InsP_3R$ Abs was at the background level. When the immunopurified anti-$InsP_3R$ Abs preadsorbed with the purified antigen were used, the label, both in Purkinje cells and other regions of cerebellar cortex, was not different from background.

For the quantitative evaluation of $InsP_3R$ distribution, particles were counted within a space extending 20 nm from either surface of the membranes of the various analyzed structures. These counts were made in a group of randomly selected pictures obtained from sections processed under standard conditions, and background was subtracted. To express the data in terms of $InsP_3R$ relative density in the various membranes, they were normalized to the length of membrane profiles in each analyzed structure. Areas and profile lengths were measured by means of a Zeiss MOP1 apparatus.

Results

Immunofluorescence

The cerebellar cortex of adult rats was systematically investigated. Immunofluorescence labeling of 1-μm-thick cryosections with anti-$InsP_3R$ Abs revealed intense labeling restricted to Purkinje cells (Fig. 1). Granule, stellate, and basket cells were not labeled by the Abs. Within the Purkinje cells, labeling was cytoplasmic. In the cell body the distribution was spotty, with some preference for both the subplasmalemmal region and the deep cytoplasm surrounding the nucleus. Dendrites were more heavily labeled than cell bodies and label extended, with similar intensity, up to the small arborizations. High-power photomicrographs revealed labeling of

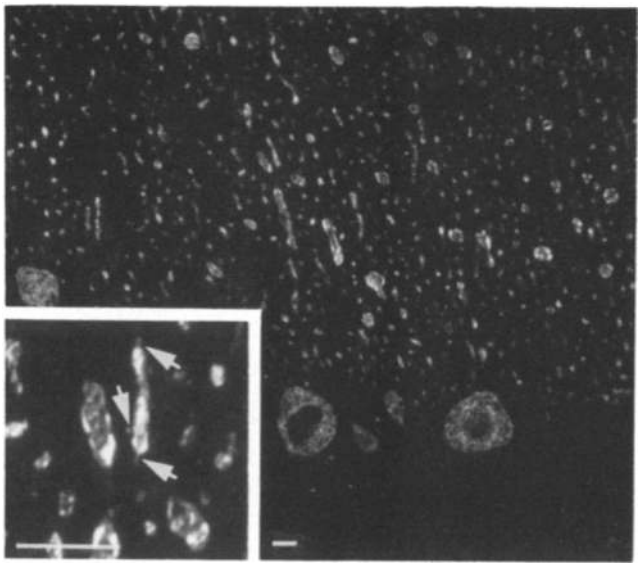

Figure 1. Immunofluorescence labeling of a 1-μm-thick rat cerebellar cortex sections with anti-$InsP_3R$. $InsP_3R$ is revealed exclusively in Purkinje cells, at both the large cell body (localized at the boundary between the granular and the molecular layer) and the intricate dendritic arborization (in the molecular layer). The high-power inset shows that dendrites are labeled not only in their shaft but also in the spines. Cerebellar granules and the cells of the molecular layer (stellate and basket cells) appear negative. Bars, 10 μm.

dendritic spines, appearing as small bodies contiguous with dendrites (Fig. 1, *inset*). These results at the light level are consistent with those both we and others have reported using thicker sections labeled by either immunoperoxidase (Ross et al., 1989; Maeda et al., 1989) or immunofluorescence (Mignery et al., 1989).

Immunogold: The Cell Body

We examined the ultrastructure of the Purkinje cell body cytoplasm in both conventional (Epon embedding, Fig. 2, *A–C*) and $InsP_3R$ Ab immunogold-labeled ultrathin frozen sections (Figs. 2 *D*, 3 and 4). The two types of preparations were investigated in parallel to help identify structures in cryosections by directed comparison with their conventional counterparts. To this end, the experimental conditions were kept as uniform as possible; in particular, the conventional thin sections were cut from blocks of cerebellar tissue fixed initially by intracardiac perfusion with 4% paraformaldehyde-0.2% glutaraldehyde, i.e., with the mild fixative solution used to preserve immunoreactivity of cryosections. Under these conditions areas of focal swelling appeared, most often located in the Golgi area, near the nuclear envelope and adjacent to ER cisternae and cisternal stacks. The rest of the cytoplasm, however, appeared well preserved, occupied by closely packed organelles (Fig. 2 *A*). As described previously (Palay and Chan-Palay, 1974), rough-surfaced ER cisternae, often heavily studded with ribosomes, were distributed either parallel to each other or were more disordered. Cisternae without attached ribosomes were also numerous, often arranged in stacks. The stacks comprised multiple (up to 12) parallel flat cisternae separated by spaces of uniform thickness, occupied by perpendicular bridges, regularly spaced at ≈25 nm (center-to-center) from each other, as revealed by both cross and grazing sections (Fig. 2, *B* and *C*). Cisternal stacks were distributed throughout the cytoplasm (Fig. 2 *A*), with some concentration in the subplasmalemmal region where smooth cisternal singlets and doublets (the latter often without appreciable intercisternal bridges) were also located (hypolemmal cisternae, Rosenbluth, 1962). Sometimes the cisternal stacks were in close apposition to mitochondria (Fiori and Mugnaini, 1981).

The relationship between rough-surfaced and stacked cisternae was investigated in some detail. In a population of 160 stack profiles from seven randomly selected Purkinje cells, 44.5% (often, but not always located beneath the plasmalemma) failed to exhibit any attached ribosomes. In the remaining profiles (55.5%), ribosomes, although excluded from the deep membranes (i.e., those bearing the regularly spaced bridges) were present at the stack surface. In many cases ribosomes were seen covering (completely or, more often, only in part) the free face of one (27%) or both (12%) superficial cisternae (Fig. 2 *A*, *short arrows*). Direct membrane (and thus lumenal) continuity between one or (at the most) two stacked cisternae and typical rough ER cisternae, studded with ribosomes on both their surfaces, was observed in 19.5% of the profiles (Fig. 2, *A* and *C*, *long arrows*). In a few profiles (5%), both surface ribosomes and continuity with rough ER cisternae were observed. In addition to the stacks, smooth vesicles and irregular tubules were also numerous. Continuities between tubules and rough-surfaced cisternae were also seen. In addition to these structures many other organelles were recognized in Purkinje cells, including numerous mitochondria (Fig. 2 *A*), a well-developed Golgi complex, and multivesicular bodies. In $InsP_3R$-Ab gold-labeled cryosections, the structures described in the conventional sections were easily recognized and their labeling varied considerably. Except for the areas with tissue swelling, which were often artefactually decorated (*asterisks* in Figs. 2 *D*, 3 *B*, and 4 *A*), the labeling was highly specific. In mitochondria (Figs. 2 *D*, 3, *A* and *C*), nucleus (Fig. 3 *A*), multivesicular bodies (Fig. 2 *D*), and at the regions of the plasmalemma not immediately adjacent to labeled cisternae, the number of gold particles was consistently low, at the level estimated as the background. The Golgi complex was also unlabeled, except for a few tubules and vesicles (not shown). Slightly higher labeling was observed over perinuclear (Fig. 3 *A*) and rough ER cisternae (Figs. 2 *B* and 3 *A*). In the latter structures, gold particles appeared usually concentrated at discrete sites (*arrows* in Fig. 3 *A*). Moreover, several rough ER cisternae as well as the external perinuclear membrane were seen in direct membrane continuity with apparently smooth structures (vesicles or irregular tubular profiles), exhibiting considerable labeling (Fig. 3 *B*). Additional poorly defined structures scattered around in the cytoplasm were also positive, sometimes to a considerably high degree. The most consistent labeling, however, occurred in two additional cytoplasmic components, smooth cisternal stacks and hypolemmal cisternae. At these structures, the gold particles were clearly distributed at both membrane surfaces, as it is to be expected from the immunolabeling of a large, transmembrane protein molecule expressing immunogenic sites on both surface domains. The majority of the >200 stacks observed were labeled in most cisternae (Figs. 2 *B* and 4 *A*), although not uniformly. In fact, the gold particles appeared

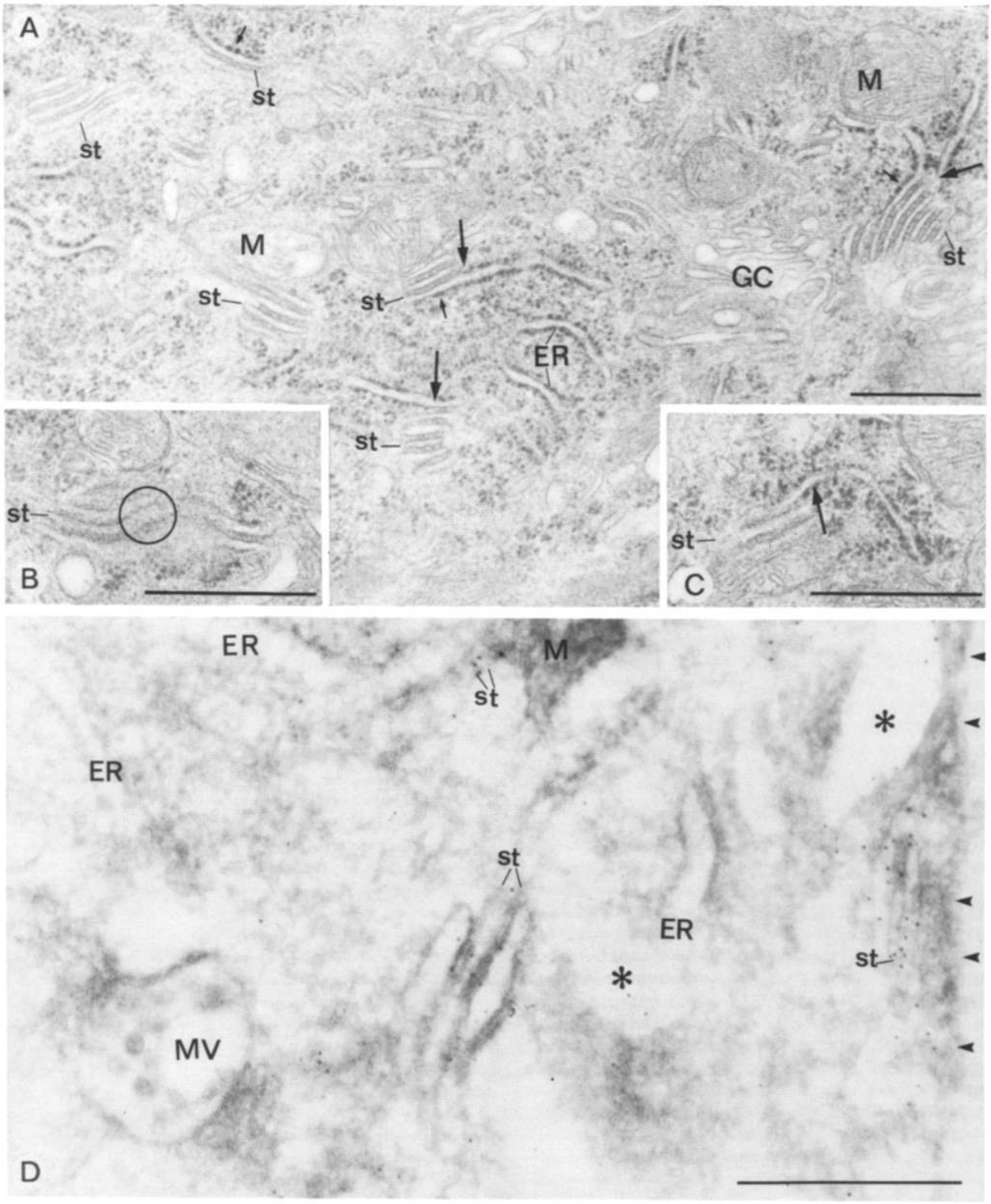

Figure 2. Conventional EM (*A–C*) and $InsP_3R$ immunogold labeling (*D*) of the Purkinje cell body. The structure of various organelles is illustrated in *A–C*: mitochondria (*M*), rough-surfaced ER cisternae (*ER*), and Golgi complex (*GC*). Stacks of parallel smooth-surfaced cisternae separated by regularly spaced (25 nm center to center) bridges are labeled *st*. A front view of the bridges (grazing section of stacked cisternae) is shown encircled in *B*. Individual cisternae of some of the stacks appear lumenally continuous with recognizable rough-surfaced ER cisternae (*big arrows* in *A* and *C*). In other stacks, the superficial cisternae are covered with ribosomes on part of their free surface (*small arrows*). *N*, nucleus. *D* shows that $InsP_3R$ is localized primarily on the membrane of stacked cisternae, (*st*) both in the deep cytoplasm and beneath the plasma membrane. Note lack of label on plasma membrane (*arrowheads*), mitochondria (*M*), and a multivesicular body (*MV*). The gold labeling of the swollen area (*) is artifactual. Other marks as in *A*. Bars, 0.5 μm.

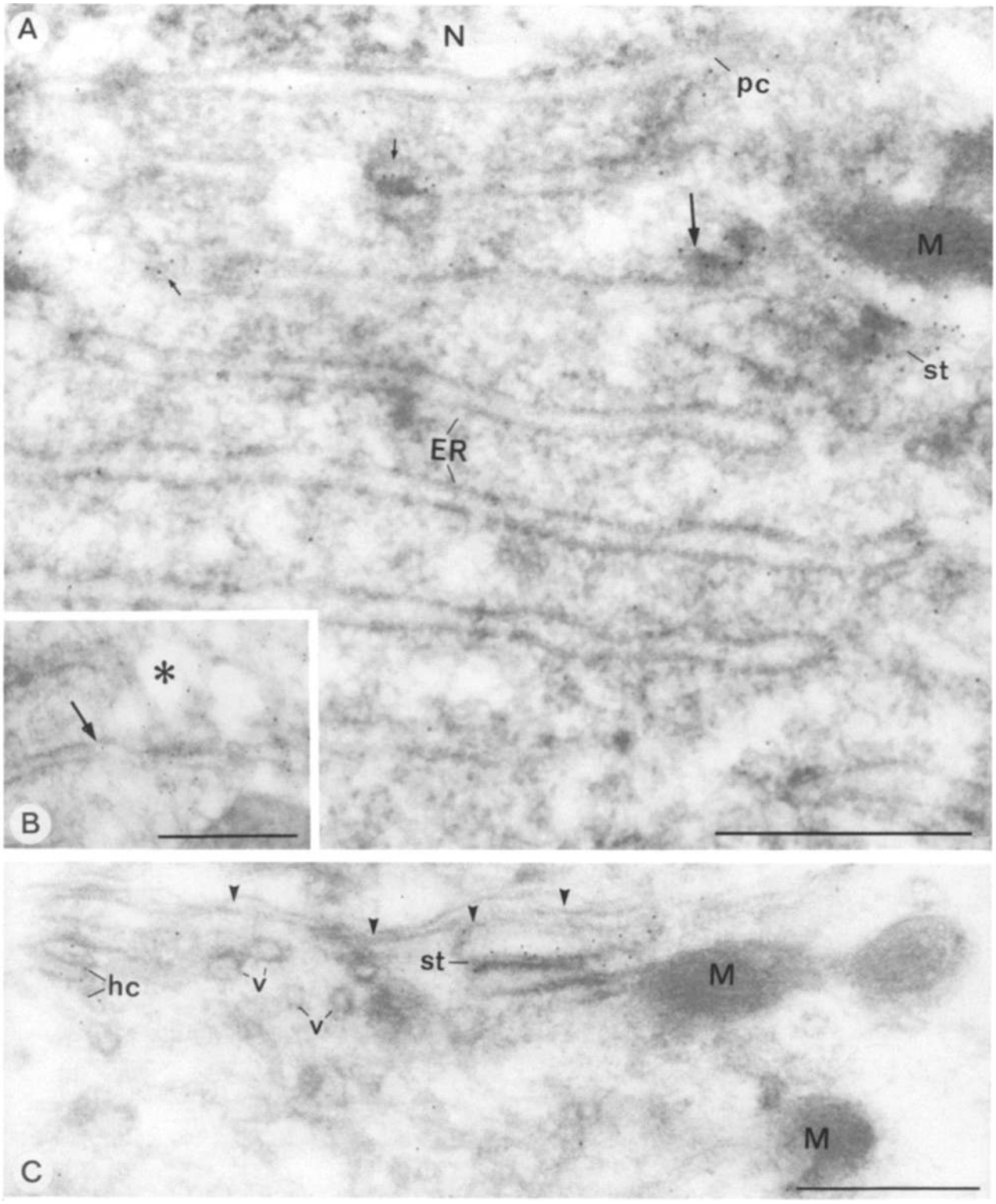

Figure 3. $InsP_3R$ immunogold labeling of the Purkinje cell body. *A* shows that the perinuclear (*pc*) and rough-surfaced ER cisternae are themselves little labeled but can be continuous (*big arrow*) with highly labeled structures, including cisternal stacks (*st*) or apparently smooth cisternae and twisted tubules. The small arrows point to clusters of immunogold particles over ER cisternae, possibly the sites of lumenal continuities with other structures. Continuity (*big arrow*) between a rough-surfaced cisterna and an $InsP_3R$-labeled, irregular smooth-surfaced structure is shown in *B*. *C* illustrates the distribution of the labeling in the cytoplasmic region near the cell surface. Both the plasma membrane (*arrowheads*) and adjacent vesicular profiles (*v*) appear unlabeled, whereas the two small multicisternal structures, localized at the center and to the left (one with evident intermembrane dense material [*st*], the other without [*hc*]) are labeled. Other marks as in Fig. 2. Bars, 0.5 μm.

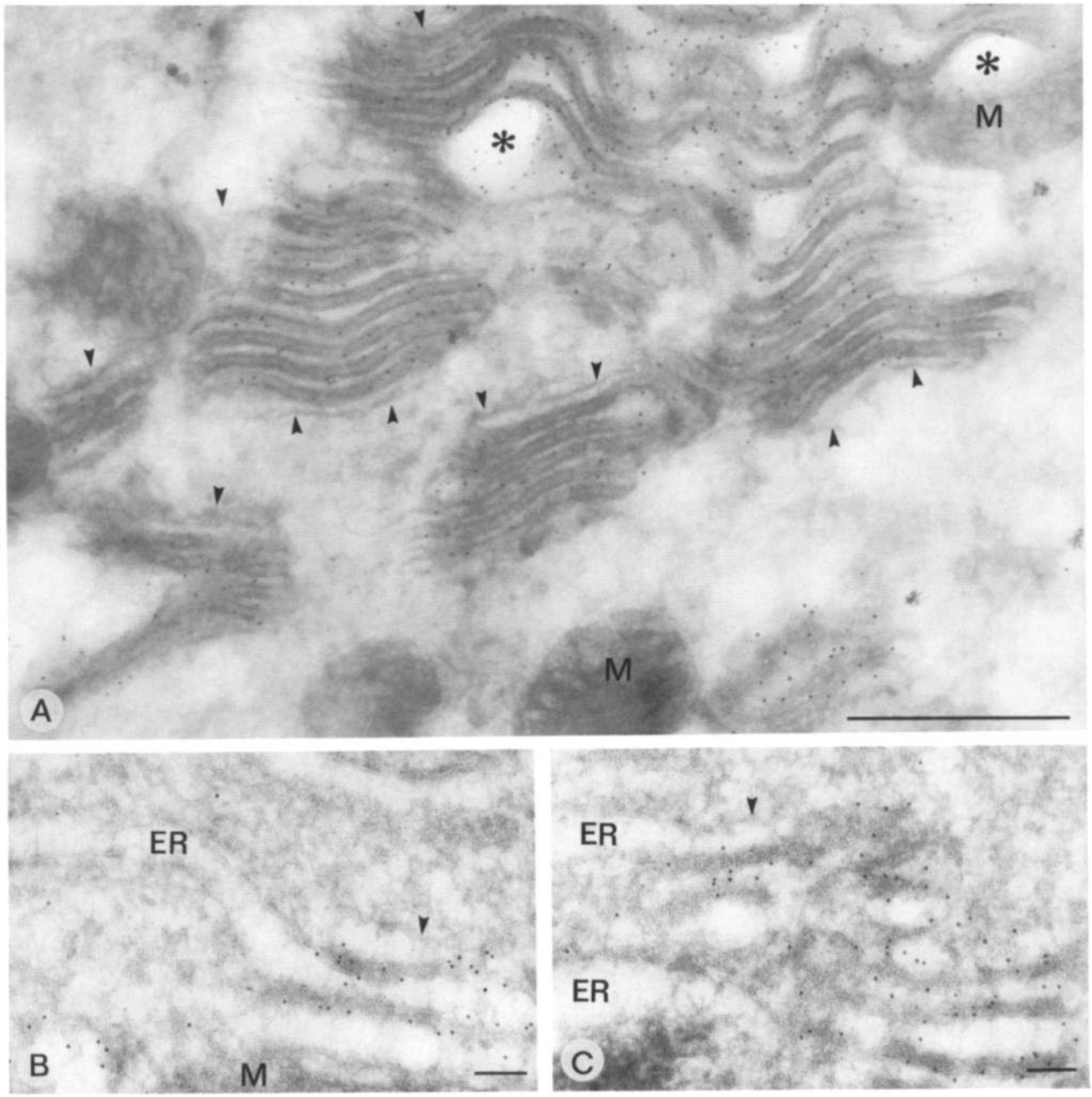

Figure 4. $InsP_3R$ immunogold labeling of cisternal stacks within the Purkinje cell body. *A* shows an unusually high concentration of large, typical stacks, all of which labeled, although not to a uniform degree. Notice that in most cases the gold particles appear distributed at the membrane portions facing the intercisternal bridges, which in cryosections appear as a dense filamentous material, while the cytosolic surfaces of the stacks (*arrowheads*) are often free of labeling. Asterisks label artifactually gold-decorated swellings of the cryosection. *B* and *C* illustrate at high magnification the lumenal continuity of stacked cisternae with rough-surfaced ER cisternae and, within the stacks, the preferential distribution of the gold particles at the membrane regions adjacent to the dense filamentous material in between the cisternae. Notice that in both panels the stack superficial cisternal faces (*arrowheads*) are unlabeled. Other marks as in Fig. 2. Bars: (*A*) 0.5 μm, (*B* and *C*) 0.1 μm.

most often concentrated in the membrane regions directly adjacent to the regularly spaced bridges in between the stacked cisternae, whereas the free surfaces were little labeled. In the cryosections the bridges were poorly resolved and usually appeared as a dense, filamentous material (Fig. 4, *A–C*). Only in a few stacks the degree of gold labeling of the various cisternae was uneven (some gradient distribution from top to bottom, Fig. 4 *A*). The rough-surfaced cisternae in continuity with individual stacked cisternae appeared much less labeled or completely unlabeled (Figs. 3 *A*, 4, *B* and *C*). Beneath the plasma membrane, multiple cisternal stacks as well as individual or coupled hypolemmal cisternae were heavily labeled, closely resembling those located more deeply in the cytoplasm (Fig. 3 *C*). Some of these labeled cisternae were located en face of a synaptic terminal impinging onto the plasma membrane (not shown). Other subplas-

Table I. Specific $InsP_3R$ Immunogold Labeling of Intracellular Structures of the Purkinje Cell Body

Structure	No. of analyzed structures	Total membrane length	Gold particles/ μm membrane profile*
		μm	
Rough ER cisternae	398	293.4	0.56 ± 0.35
Perinuclear cisternae	15	75.4	0.42 ± 0.26
Hypolemmal cisternae‡	23	21.8	2.80 ± 1.3
Cisternal stacks‡	107	255.3	5.82 ± 2.2

* Averages ± SD. Gold particles lying within 20 nm from each membrane surface were counted. 1 μm profile corresponds therefore to 0.04 μm^2 area. Values shown were subtracted of the background (4.8 particle/μm^2), calculated over parallel cryosections processed for immunogold labeling but using the preimmune serum, and corresponding to the values measured over mitochondria and nucleus in the $InsP_3R$-immunodecorated Purkinje cells cryosections. ‡ Only single and double cisternae located adjacent to the plasma membrane and exhibiting no prominent dense, intercisternal filamentous material were grouped as hypolemmal cisternae. Subplasmalemma stacks with obvious dense filamentous material were grouped together with those located deep in the cytoplasm.

malemma cisternae, however, were little labeled or completely negative. Smaller structures located beneath the plasma membrane, sometimes recognizable as coated vesicles, were usually unlabeled (Fig. 3 *C*).

Quantitative analyses by direct counting of gold particles further confirmed the results described above. In a group of 15 pictures chosen at random, exhibiting a total of >2,000 gold particles, recognizable stacks and hypolemmal cisternae were found to account for the 55% of the labeling in the Purkinje cell body. On the other hand, the specific labeling of cisternal stacks (expressed in terms of membrane profile length) was 10-fold greater than that of rough-surfaced ER and perinuclear cisternae, with labeling of the latter structures being 2–3-fold background. Values for hypolemmal cisternae were intermediate between stacks and rough ER cisternae (Table I).

Immunogold: The Dendrites

In agreement with the immunofluorescence data, the Purkinje cell dendrites were heavily immunogold positive for the $InsP_3R$, irrespective of their size and location in the molecular layer. In most cases over half of the discernible membrane-bound structures (compare Fig. 5, *A* and *B*): tubules, cisternae (often arranged as couples or triplets, located both beneath the plasma membrane and in the deep regions), and vesicles were labeled, although not always with uniform intensity. Additional structures, similar in size, shape, and distribution, were unlabeled (Fig. 5 *B*). Typical stacks, with regularly spaced bridges in between adjacent parallel cisternae, were usually smaller than in the cell body (compare Figs. 5 *A* and 2 *A*). They were often wrapped around or closely apposed to a mitochondrion, and were heavily labeled (Fig. 5 *C*). Cisternal piles, less precisely arranged compared with typical stacks, were variably labeled (Fig. 5 *C*). Dendritic spines were hard to investigate, because most of them apparently fell off the cryosections during processing. 13 spines were identified in our preparations, and all were $InsP_3R$-positive, with labeling restricted to the internal smooth membrane-bound structure: tubules and cisternae, often organized in doublets or triplets, however, without discernible interposed bridges (Fig. 5 *D*). No immunolabeling was observed at the plasma membrane or the postsynaptic density area (Fig. 5 *D*).

Discussion

In this work, immunogold labeling of ultrathin cryosections has been used to establish the intracellular distribution of $InsP_3R$ in Purkinje cells. The highest concentration (up to 50-fold the background level) was found in a population of smooth-surfaced structures (cisternae often arranged in piles or stacks, tubules, and possibly vesicles) distributed both near the surface and within the cell body and the dendrites, up to the dendritic spines. These structures were often seen in direct continuity with membranes of rough-surfaced ER and also with the perinuclear cisterna, which by themselves were much less intensely labeled (two- to threefold the background). Finally, other organelles and structures, including mitochondria and the plasma membrane, were not labeled above background.

These findings extend and qualify the results of our previous studies, carried out primarily by immunoperoxidase, using the same Ab here (Ross et al., 1989). In those studies a population of rough and smooth-surfaced ER elements, as well as the nuclear envelope, appeared considerably labeled, whereas other ER elements (together with mitochondria and the plasmalemma) were clearly negative. The discrepancy between these data and those obtained in this work might be only apparent, depending on the different experimental approach used. In fact, immunoperoxidase results are hard to interpret in quantitative terms and possess a lower spatial resolution compared with immunogold. The different levels of $InsP_3R$ expression, now revealed by immunogold, between smooth- and rough-surfaced ER elements could thus have been difficult to appreciate in the peroxidase specimens, especially if some degree of redistribution of the peroxidase-generated dense precipitate across the lumenal continuities between the two types of structures had induced a partial homogenization of their labeling. The possibility that the differences observed with the two techniques were due to the fixatives used (formaldehyde alone for immunoperoxidase; formaldehyde plus 0.2% glutaraldehyde for immunogold) was ruled out by experiments carried out by the latter technique in formaldehyde-fixed samples, with no appreciable differences of the labeling distribution compared to the results herewith described (not shown).

Our results should also be compared with those obtained using other Abs to the $InsP_3R$ protein. In their immunoperoxidase studies, Maeda et al. (1989) observed labeling of not only the ER but also the plasma membrane, in particular near postsynaptic densities. In no case did we observe any specific labeling of these structures, even when organelles in their proximity, such as hypolemmal cisternae and the cisternal apparatus within the spines, were densely labeled. The absence of the receptor from the plasma membrane revealed by our results correlates well with the lack of Ca^{2+} influx when most cell types (except lymphocytes and mast cells) are microinjected with $InsP_3$ (for a recent review see Berridge and Irvine, 1989). Another study on $InsP_3R$ (Mignery et

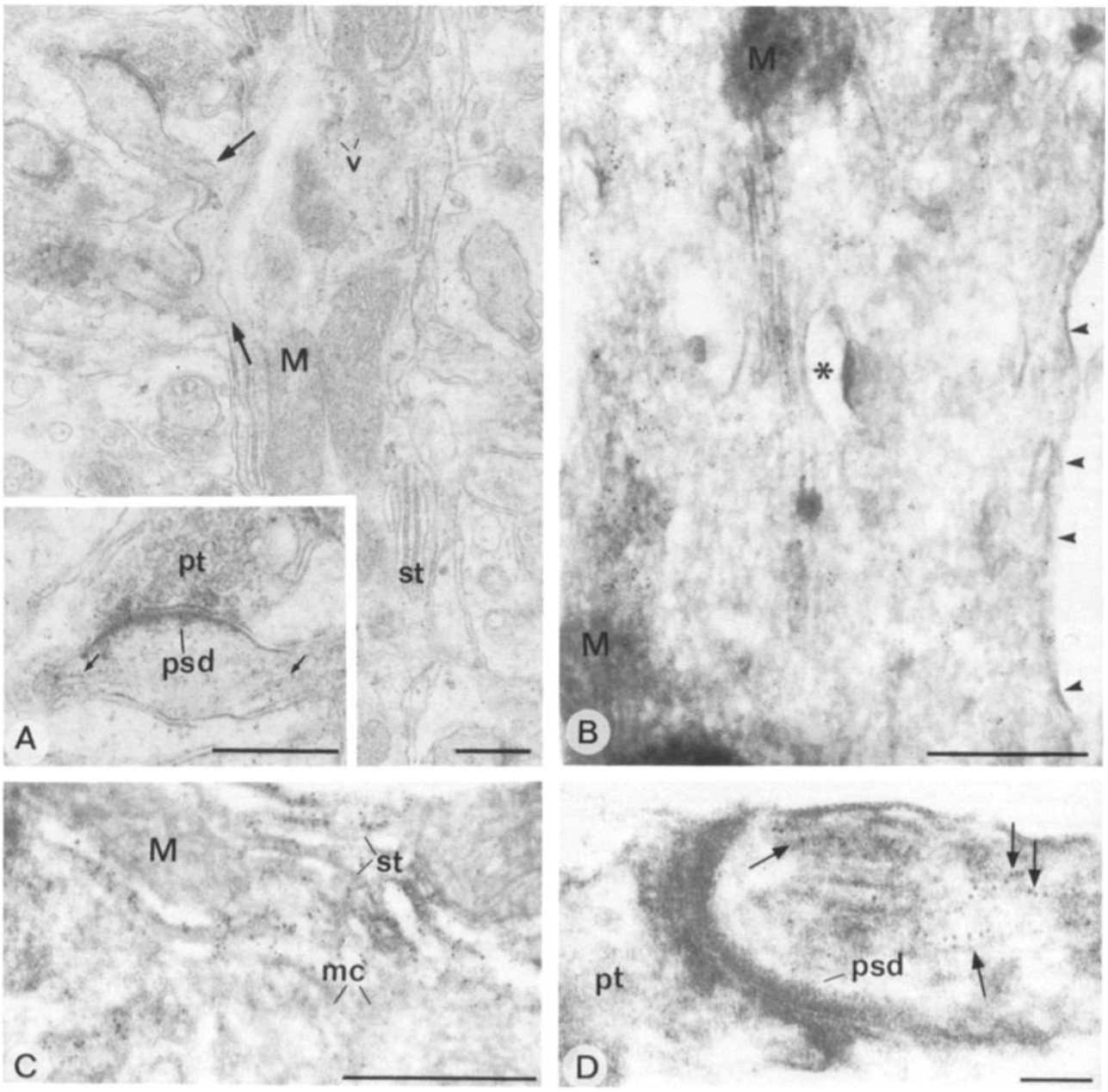

Figure 5. Conventional microscopy and $InsP_3R$ immunogold labeling of Purkinje cell dendrites. The conventional image of a (longitudinally oriented) dendrite, shown in *A*, illustrates the membrane-bound structures distributed both in the shaft and in the spines. Notice the relatively small cisternal stacks (*st*) and numerous mitochondria (*M*) present in the shaft together with individual cisternae and vesicles (*v*). The origin of spines is indicated by arrows and one of them, enlarged in the inset, exhibits a few parallel cisternae oriented along the main axis (*arrows*). The cryosection in *B* shows that many (but not all) smooth cisternae and vesicular profiles of the shaft are labeled. They are located both beneath the plasma membrane (*arrowheads*) and in the internal regions. *C* illustrates a typical cisternal stack (*st*) wrapped around a mitochondrion (*M*). Of the two apparently discrete membrane clusters (*mc*), that at center is moderately labeled, that to the right is almost unlabeled. *D* shows a dendritic spine, recognizable by its shape and participation in synapse. Notice the labeling of various longitudinal cisternae, the spine apparatus (*arrows*). *psd*, postsynaptic density; *pt*, presynaptic terminal. *Artifactual swellings. Bars: (*A–C*) 0.5 μm, (*D*) 0.1 μm.

al., 1989) was carried out by immunogold labeling. In agreement with our present findings, these authors observed negative mitochondria and plasma membrane as well as intense labeling of smooth-surfaced ER cisternae and tubules, including subplasmalemma cisternae, cisternal stacks, and the spine cisternal apparatus. However, probably because of the technique primarily used (immunolabeling of agarose-embedded tissue fragments), Mignery et al. (1989) failed to observe continuities of the labeled smooth structures with rough-surfaced cisternae and to appreciate the intense labeling of the stacked membranes. In fact, membrane continuities might have become discontinued during the mild homogenization applied to the tissue to generate fragments, whereas the presence of bridges in between adjacent stacked cisternae most likely prevented the access of the Abs to the $InsP_3R$ now revealed in our cryosections.

A question that might be asked concerns the nature of the $InsP_3R$-positive organelles, in particular that of the cisternal stacks expressed by the Purkinje cells. So far these structures have been investigated to a very limited extent and only by morphological techniques (Rosenbluth, 1962; Mignery et al., 1989). However, our present observation that >50% of the stack profiles are either partially covered with ribosomes at their free surface or exhibit membrane continuities with bona fide rough ER cisternae appears to meet a widely accepted criterion of attribution to the ER. Within that membrane system the $InsP_3R$-enriched structures appear to constitute a highly specialized, smooth-surfaced, subcompartment. This conclusion appears in general agreement with the results of numerous subfractionation studies that showed only part of the microsomal fraction to be sensitive to the second messenger (Prentki et al., 1984; Henne et al., 1987; Krause and Lew, 1987; Volpe et al., 1988; Rossier et al., 1989; Thevenod et al., 1989; Ghosh et al., 1989). However, working with different cell types, the $InsP_3$ sensitivity was sometimes recovered in the light, mostly smooth surfaced (Henne et al., 1987; Krause and Lew, 1987; Volpe et al., 1988), and sometimes in the heavy, mostly rough-surfaced (Prentki et al., 1984; Ghosh et al., 1989) subfraction.

Although in our cryosections, the density of immunogold labeling was moderate even in the cisternal stacks, based on the higher values observed in cerebellar homogenates by Mignery et al. (1989) and on the quantitation criteria discussed by Griffiths and Hoppeler (1986) the receptor concentration in the internal membranes of the stacks can be predicted to be high. Recent studies (Furuichi et al. 1989; Mignery et al., 1989; Maeda et al., 1990) have revealed a considerable degree of molecular homology and structural similarity between the $InsP_3R$ and the ryanodine receptor. The latter is the Ca^{2+} channel concentrated in the membrane of the muscle sarcoplasmic reticulum terminal cisternae, where it accounts for the discrete particles bridging the triad gap, the so-called junctional feet. In conventional thin sections, feet appear as regularly spaced bridges (Somlyo, 1979; Franzini-Armstrong and Nunzi, 1983), similar to those observed in between our stacked cisternae. Based on this similarity and on the recently reported geometry of the $InsP_3R$ (Maeda et al., 1990), the possibility should be considered that the regularly spaced bridges of the stacks are composed by receptor molecules, possibly arranged in register in the adjacent membranes. Whether the $InsP_3R$ in the stacks, which constitute a large fraction of the huge complement of Purkinje cells, are functional or not is not clear at the moment. In case receptors are not functional, the stacks could serve not as a Ca^{2+} store but as a reservoir for $InsP_3R$, which could be quickly redistributed to the other $InsP_3$-sensitive organelles, in both the cell body and the dendrites.

As discussed extensively elsewhere (Volpe et al., 1988; Hashimoto et al., 1988), for Ca^{2+} storage organelles to be fully functional they need to express not only a regulated Ca^{2+} channel (in this case, the $InsP_3R$), but also a Ca^{2+} pump (in their membrane) and an appropriate, low-affinity, high-capacity Ca^{2+}-binding protein (within their lumen). A Ca^{2+}-ATPase is largely expressed in Purkinje cells (Kaprelian et al., 1989). So far, immunofluorescence experiments carried out with Abs against low-affinity, high-capacity Ca^{2+}-binding proteins (muscle calsequestrin [Volpe et al., 1988]; liver calreticulin [Treves et al., 1990]) yielded negative results in Purkinje cells. At the moment, therefore, we do not know whether all the $InsP_3R$-positive organelles (or only some of them) express an appropriate Ca^{32+} storage protein in their lumen. This appears to be highly probable, however, for at least the spine cisternae, since they were found by electron probe microanalysis to accumulate large amounts of Ca^{2+}, especially after depolarization with high K^+ (Andrews et al., 1988). Thus, it is possible that Purkinje cells express a low-affinity, high-capacity Ca^{2+}-binding protein different from that located in the other neurons and peripheral cells.

The high concentration of $InsP_3R$ that we have detected in the dendrites, in particular at the level of spines, corresponds to sites for glutamatergic synapses derived from cerebellar granule cells via the parallel fibers. These synapses appear to activate quisqualate-preferring ACPD glutamatergic receptors coupled to phosphatidylinositol-4,5-bisphosphate hydrolysis, and thus to $InsP_3$ generation (Nicoletti et al., 1986; Ambrosini and Meldolesi, 1989; Blackstone et al., 1989). Moreover, in hippocampal neurons, activation of these receptors by quisqualate triggers intracellular Ca^{2+} release (Murphy and Miller, 1988; Mayer and Miller, 1990). In contrast, synapses impinging onto the Purkinje cell body from basket and stellate cells are believed to be GABA-ergic, opening Cl^- channels rather than inducing $InsP_3$ generation. Thus, whether the $InsP_3R$-positive cisternae located in the cell body beneath the plasma membrane, just in front of impinging terminals, are located strategically in relation to synaptic transmission is still unclear.

In conclusion, we have demonstrated that in cerebellar Purkinje cells, the $InsP_3R$ is highly concentrated in smooth-surfaced elements, especially, but not exclusively, cisternae. These cisternae are often, but not always, arranged in stacks, which may be in direct membrane continuity with the rest of the ER. In Purkinje cells, the $InsP_3$-sensitive compartment appears therefore to be neither distinct from the ER, as hypothesized in other cell types (Volpe et al., 1988) nor to coincide with this entire endomembrane system. Further studies are needed to establish whether the heterogeneity of this subcompartment with respect to the rest of the ER is limited to the high concentration of $InsP_3R$ or concerns other components as well.

We are grateful to S. Balsari and S. Monti for technical and secretarial assistance, respectively. This work was supported by grants from the Consiglio Nazionale delle Ricerche (Strategic Project Transmembrane Signaling and Special Project Biotechnology and Bioinstruments); U.S. Public Health Service grant MH-18501; and by a gift of Bristol-Myers-Squibb. C. A. Ross is supported by National Institute of Mental Health grant MH-43040, and is a Peer Scholar in the Biomedical Sciences. S. H. Snyder is the recipient of Research Scientist Award DA-00074.

Received for publication 23 January 1990 and in revised form 11 April 1990.

References

Ambrosini, A., and J. Meldolesi. 1989. Muscarinic and quisqualate receptor-induced phosphoinositide hydrolysis in primary cultures of striatal and hippocampal neurons. Evidence for differential mechanisms of activation. *J. Neurochem.* 53:825–833.

Andrews, B. S., R. D. Leapman, D. M. D. Landis, and T. S. Reese. 1988. Activity-dependent accumulation of calcium in Purkinje cell dendritic spines. *Proc. Natl. Acad. Sci. USA.* 85:1682–1685.

Berridge, M. J., and R. F. Irvine. 1989. Inositol phosphates and cell signaling. *Nature (Lond.).* 34:197–205.

Blackstone, C. D., S. Supattapone, and S. H. Snyder. 1989. Inositolphospholipid-linked glutamate receptors mediate cerebellar parallel-fiber-Purkinje-

cell synaptic transmission. *Proc. Natl. Acad. Sci. USA.* 86:4316–4320.
Ferris, C. D., R. L. Huganir, S. Supattapone, and S. H. Snyder. 1989. Purified inositol 1,4,5-trisphosphate receptor mediates calcium flux in reconstituted lipid vesicles. *Nature (Lond.).* 342:87–89.
Fiori, M. G., and E. Mugnaini. 1981. Subsurface and cytoplasmic cisterns associated with mitochondria in pyramidal neurons of the rat dorsal cochlear nucleus. *Neuroscience.* 6:461–471.
Franzini-Armstrong, C., and G. Nunzi. 1983. Junctional feet and membrane particles in the triad of a fast twitch muscle fiber. *J. Muscle Res. Cell Motil.* 4:233–252.
Furuichi, T., S. Yoshikawa, A. Miyawaki, K. Wada, N. Maeda, and K. Mikoshiba. 1989. Primary structure and functional expression of the inositol 1,4,5-trisphosphate-binding protein P_{400}. *Nature (Lond.).* 342:32–38.
Ghosh, T. K., J. M. Mullaney, F. I. Taranzi, and D. L. Gill. 1988. GTP-activated communication between distinct inositol 1,4,5-trisphosphate-sensitive and -insensitive calcium pools. *Nature (Lond.).* 340:236–239.
Griffiths, G., and H. Hoppeler. 1986. Quantitation in immunochemistry: correlation of immunogold labeling to absolute number of membrane antigens. *J. Histochem. Cytochem.* 34:1389–1398.
Groswald, D. E., and P. T. Kelly. 1984. Evidence that a cerebellum-enriched, synaptic junction glycoprotein is related to phodrin and resists extraction with triton in a calcium-dependent manner. *J. Neurochem.* 42:534–546.
Guillemette, G., T. Balla, A. J. Baukal, A. Spät, and K. J. Catt. 1987*a*. Intracellular receptors for inositol 1,4,5-trisphosphate in angiotensin II target tissues. *J. Biol. Chem.* 262:1010–1015.
Guillemette, G., T. Balla, A. J. Baukal, and K. J. Catt. 1987*b*. Inositol 1,4,5 trisphosphate binds to a specific receptor and releases microsomal calcium in the anterior pituitary gland. *Proc. Natl. Acad. Sci. USA.* 84:8195–8199.
Hashimoto, S., B. Bruno, D. P. Lew, T. Pozzan, P. Volpe, and J. Meldolesi. 1988. Immunocytochemistry of calciosomes in liver and pancreas. *J. Cell Biol.* 107:2524–2531.
Henne, V., A. Piiper, and H. D. Soling. 1987. Inositol 1,4,5-trisphosphate and 5'-GTP induce calcium release from different intracellular pools. *FEBS (Fed. Eur. Biochem. Soc.) Lett.* 218:153–158.
Kaprelian, Z., A. M. Campbell, and D. M. Fambrough. 1989. Identification of a Ca^{2+}-ATPase in cerebellar Purkinje cells. *Mol. Brain Res.* 6:55–60.
Keller, G. A., K. T. Tokuyasu, A. H. Dutton, and S. J. Singer. 1984. An improved procedure for immunoelectron microscopy: ultrathin plastic embedding of immunolabeled ultrathin frozen sections. *Proc. Natl. Acad. Sci. USA.* 81:5744–5747.
Krause, K. H., and D. P. Lew. 1987. Subcellular distribution of Ca^{2+} pumping sites in human neutrophils. *J. Clin. Invest.* 80:107–116.
Maeda, N., M. Niinobe, Y. Inoue, and K. Mikoshiba. 1989. Developmental expression and intracellular location of P_{400} protein characteristic of Purkinje cells in the mouse cerebellum. *Dev. Biol.* 133:67–76.
Maeda, N., M. Niinobe, and K. Mikoshiba. 1990. Inositol 1,4,5-trisphosphate ($InsP_3$) receptor protein. Purification and characterization of $InsP_3$ receptor complex. *EMBO (Eur. Mol. Biol. Organ.) J.* 9:61–67.
Mallet, J., M. Hughet, R. Pougeois, and J. P. Changeux. 1976. Anatomical, physiological and biochemical studies on the cerebellum from mutant mice. III. Protein differences associated with the weaver, staggerer and nervous mutations. *Brain Res.* 103:291–312.
Mayer, M. L., and R. J. Miller. 1990. Excitatory amino acid receptors, second messengers and mechanisms underlying regulation of intracellular calcium in mammalian neurons. *Trends Pharmacol. Sci.* In press.
Mignery, G. A., T. C. Sudhof, K. Takei, and P. De Camilli. 1989. Putative inositol 1,4,5-trisphophate receptor similar to ryanodine receptor. *Nature (Lond.).* 342:192–195.
Murphy, S. N., and R. J. Miller. 1989. Regulation of Ca^{2+} influx into striatal neurons by kainic acid. *J. Pharmacol. Exp. Ther.* 249:184–193.
Nicoletti, F., J. T. Wroblewski, and E. Costa. 1986. Excitatory amino acid recognition sites coupled with inositol phospholipid metabolism: developmental changes and interaction with α1-adrenoceptors. *Proc. Natl. Acad. Sci. USA.* 83:1931–1935.
Palay, S., and V. Chan-Palay. 1974. Cerebellar Cortex: Cytology and Organization. Springer-Verlag, Berlin. 1–348.
Prentki, M., T. J. Biden, D. Janjic, R. F. Irvine, M. J. Berridge, and C. B. Wollheim. 1984. Rapid mobilization of Ca^{2+} from rat insulinoma microsomes by inositol-1,4,5-trisphosphate. *Nature (Lond.).* 309:562–564.
Rosenbluth, J. 1962. Subsurface cisterns and their relationship to the neuronal plasma membrane. *J. Cell Biol.* 13:405–420.
Ross, C. A., J. Meldolesi, T. A. Milner, T. Satoh, S. Supattapone, and S. H. Snyder. 1989. Inositol 1,4,5-trisphosphate receptor localized to endoplasmic reticulum in cerebellar Purkinje neurons. *Nature (Lond.).* 339:468–470.
Rossier, M. F., A. M. Capponi, and M. B. Vallotton. 1989. The inositol 1,4,5-trisphosphate-binding site in adrenal cortical cells is distinct from the endoplasmic reticulum. *J. Biol. Chem.* 264:14078–14084.
Somlyo, A. V. 1979. Bridging structures spanning the junctional gap at the triad of skeletal muscle. *J. Cell Biol.* 80:743–750.
Spät, A., P. G. Bradford, J. S. McKinney, R. P. Rubin, and J. W. Putney, Jr. 1986. A saturable receptor for ^{32}P-inositol-1,4,5 trisphosphate in hepatocytes and neutrophils. *Nature (Lond.).* 319:514–516.
Supattapone, S., P. F. Worley, J. M. Baraban, and S. H. Snyder. 1988*a*. Solubilization, purification and characterization of an inositol trisphosphate receptor. *J. Biol. Chem.* 263:1530–1534.
Supattapone, S., S. K. Danoff, A. Theibert, S. K. Joseph, J. Steiner, and S. H. Snyder. 1988*b*. Cyclic AMP-dependent phosphorylation of a brain inositol trisphosphate receptor decreases its release of calcium. *Proc. Natl. Acad. Sci. USA.* 85:8747–8750.
Thevenod, F., M. Dehlinger-Kremer, T. P. Kemmer, A. L. Christian, B. V. L. Potter, and I. Schulz. 1989. Characterization of inositol 1,4,5-trisphosphate-sensitive (IsCaP) and -insensitive (IisCaP) nonmitochondrial Ca^{2+} pools in rat pancreatic acinar cells. *J. Membr. Biol.* 109:173–187.
Treves, S., M. De Mattei, M. Lanfredi, A. Villa, M. M. Green, D. MacLennan, J. Meldolesi, and T. Pozzan. 1990. Calreticulin is a protein responsible for high capacity-moderate affinity Ca^{2+} binding within a Ca^{2+} storage compartment (calciosomes) of liver and brain. *Biochem. J.* In press.
Volpe, P., H. Krause, S. Hashimoto, F. Zorzato, T. Pozzan, J. Meldolesi, and D. P. Lew. 1988. "Calciosome", a cytoplasmic organelle: the inositol 1,4,5-trisphosphate-sensitive Ca^{2+} store of nonmuscle cells? *Proc. Natl. Acad. Sci. USA.* 85:1091–1095.
Walaas, S. I., A. C. Nairn, and P. Greengard. 1986. PCPP 260, a Purkinje cell specific cyclic AMP-regulated phosphoprotein of Mr 260.000. *J. Neurosci.* 6:954–961.
Worley, P. F., J. M. Baraban, and S. H. Snyder. 1988. Inositol 1,4,5-trisphosphate receptor binding: autoradiographic localization in rat brain. *J. Neurosci.* 9:339–346.